Monitoring alpha-synuclein oligomerization and aggregation using bimolecular fluorescence complementation assays: what you see is not always what you get.

Bryan Frey, Abdelrahman AlOkda, and Hilal A. Lashuel*

Laboratory of Molecular and Chemical Biology of Neurodegeneration, Brain Mind Institute, Faculty of Life Sciences, École Polytechnique Fédérale de Lausanne (EPFL), Lausanne, CH 1015

*To whom correspondence should be addressed: Hilal A. Lashuel, Brain Mind Institute, Swiss Federal Institute of Technology Lausanne (EPFL), Lausanne, CH-1015, Switzerland. Phone: +41 21 69 39691; Email: hilal.lashuel@epfl.ch.

Keywords:
α-synuclein, Parkinson's disease, oligomerization, aggregation, bimolecular fluorescent complementation.

Abbreviations:
α-syn: α-synuclein; **α-syn-V:** α-synuclein-full length Venus; **Vn-α-syn**: n-terminal fragment of Venus fused to the amino-terminus of α-syn; **α-syn-Vc:** c-terminal fragment of Venus fused to the carboxy-terminus of α-syn; **BiFC**: bimolecular fluorescent complementation; **PD**: Parkinson´s disease; **SEC**: size exclusion chromatography

Graphical Abstract

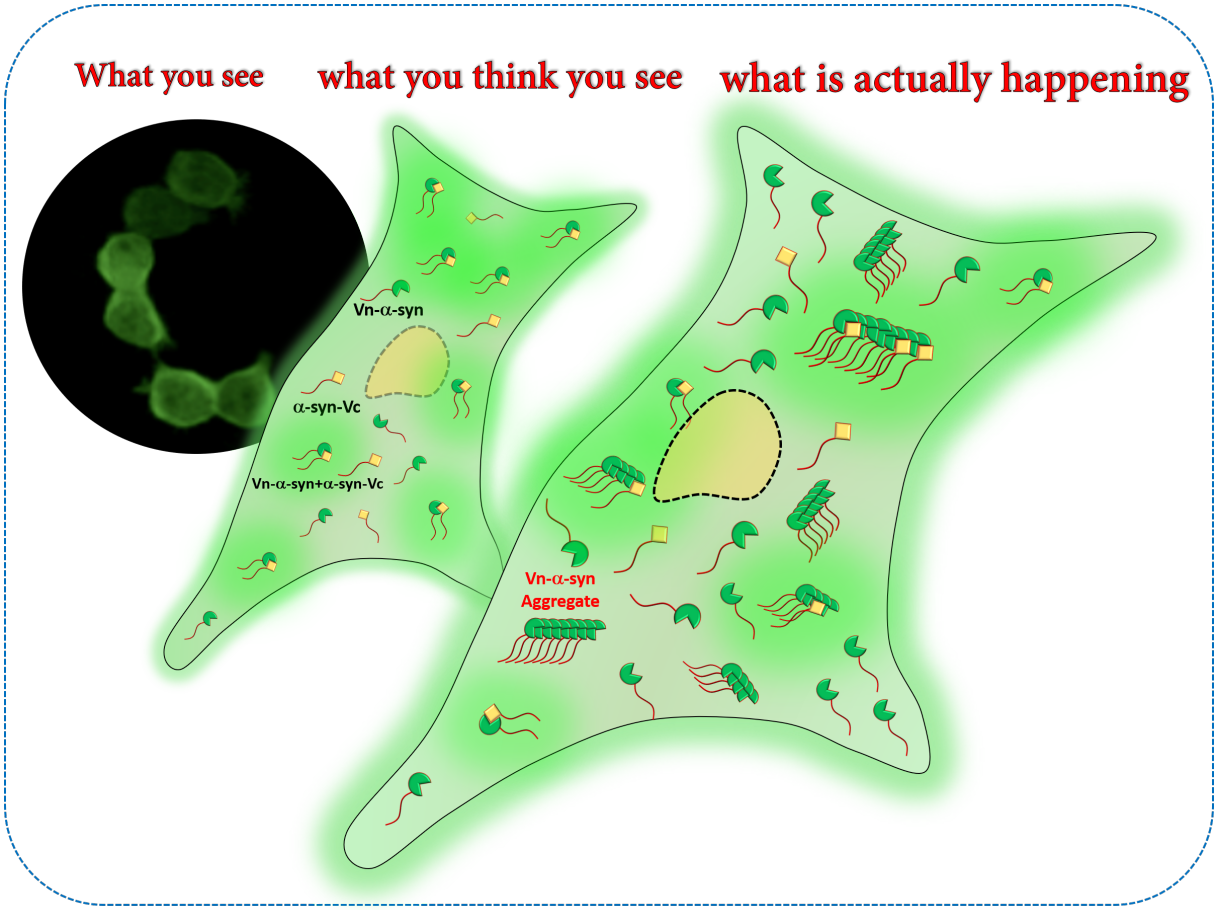

Abstract

Bimolecular fluorescence complementation (BiFC) was introduced a decade ago as a method to monitor alpha-synuclein (α-syn) oligomerization in intact cells. Since then, several α-syn BiFC cellular assays and animal models have been developed, including mouse, rat and Drosophila models, based on the assumption that an increase in the fluorescence signal correlates with increased α-syn oligomerization or aggregation. Despite the increasing use of these assays and models in mechanistic studies, target validation and drug screening, there have been no reports that 1) validate the extent to which the BiFC fluorescent signal correlates with α-syn oligomerization at the biochemical level; 2) provide a structural characterization of the oligomers and aggregates formed by the BiFC fragments; or 3) investigate the extent to which the oligomers by the fluorescent complex resemble oligomers that form on the pathway to α-syn fibrillization. To address this knowledge gap, we first analyzed the expression level and oligomerization properties of the individual constituents of α-syn-Venus, one of the most commonly used BiFC systems, in HEK-293 cells using multiple approaches, including size exclusion chromatography, semiquantitative Western blot analysis, in-cell crosslinking, immunocytochemistry and sedimentation assays. Next, we investigated the biochemical and aggregation properties of α-syn upon co-expression of both BiFC fragments. Our results show that 1) the two BiFC fragments are not expressed at the same level since C-terminal-Venus fused to α-syn (α-syn-Vc) was present in very low abundance; 2) the fragment with N-terminal-Venus fused to α-syn (Vn-α-syn) exhibited a high propensity to form oligomers and higher-order aggregates; 3) the expression of either or both fragments does not result in the formation of α-syn fibrils, cellular inclusions or the accumulation of pS129 immunoreactive α-syn aggregates. Furthermore, our results suggest that only a small fraction of Vn-α-syn is involved in the formation of the fluorescent BiFC complex and that some of the fluorescent signal may arise from the association or entrapment of α-syn-Vc in Vn-α-syn aggregates. The fact that the N-terminal fragment exists predominantly in an aggregated state also indicates that one must exercise caution when using this system to investigate α-syn oligomerization in cells or in vivo. Altogether, our results suggest that oligomerization, aggregation and cell-to-cell transmission assays and model systems based on α-syn BiFC systems should be thoroughly characterized at the biochemical level to ensure that they reproduce the process of interest and measure what they are intended to measure.

Introduction

α-Synuclein (α-syn) is a soluble protein that is highly expressed in neurons of the central nervous system (Fauvet et al., 2012; Lashuel, Overk, Oueslati, & Masliah, 2012). It is a member of the synuclein family of proteins, which includes two other shorter proteins, namely, β-syn and γ-syn (Fig. 1). Although the three proteins share significant sequence homology, only α-syn has been shown to accumulate in aggregated and fibrillar forms in Lewy bodies (LBs)and Lewy Neurites (LNs), which are the pathological hallmarks of Parkinson's disease (PD) and other neurodegenerative diseases, including Alzheimer's disease, dementia with Lewy bodies and multiple system atrophy (Goedert, Jakes, & Spillantini, 2017). Under physiological conditions, α-syn shuttles between different organelles and exists in multiple conformations depending on its localization and interactions with other proteins, lipids and membranes (Sulzer & Edwards, 2019). The transition of α-syn from its native state to its pathological forms requires it to undergo major conformational and quaternary structural changes involving a transition from disordered monomers to oligomers comprising mixed secondary structures to β-sheet rich fibrillar aggregates (Fig. 2B). Several cellular and animal models that reproduce different aspects of α-syn aggregation and pathology formation have been developed (M.-B. Fares et al., 2016; Lee & Lee, 2002; Reyes et al., 2014; Volpicelli-daley et al., 2011). However, the lack of tools that enable monitoring of the early events associated with α-syn misfolding and oligomerization has limited the utility of these models in investigating the molecular and cellular determinants of α-syn oligomer formation and toxicity. Increasing evidence suggests that targeting early aggregation events and inhibiting α-syn oligomerization represents one of the most effective strategies for preventing α-syn pathology formation and treating PD. The first step towards achieving this goal is the development of cellular and animal models in which such early oligomerization events could be visualized and quantified. Despite the development of several antibodies that have been reported to specifically detect α-syn oligomers, but not monomers or fibrils, none of these antibodies has emerged as a validated oligomer-specific or robust tool for monitoring and quantifying α-syn oligomerization in cellular models. Although several groups have reported the development and application of different assays to quantify α-syn oligomers, the great majority of these assays do not differentiate between the different aggregation states of α-syn (oligomers vs fibrils) or capture the diversity of α-syn oligomers and aggregates.

To allow monitoring of early oligomerization events (dimerization) involving α-syn in living cells, Outeiro *et al.* developed an α-syn bimolecular fluorescent complementation (BiFC) assay (Outeiro et al., 2008). The main principle behind this assay is the fusion of N- and C-terminal fragments of a reporter protein (e.g., GFP or YFP) to the proteins of interest, which in this case are α-syn monomers. These fragments are not fluorescent when they are separated and only emit a fluorescence signal if the two fragments are brought into close proximity to enable their association and the reconstitution of the structure of the full-length fluorescent protein; in this case, this occurs upon α-syn dimerization or oligomerization (Fig. 2A) (Kerppola, 2006, 2008). It is worth pointing out that BiFC was initially developed to study heterodimeric protein interactions (Hu et al., 2002; Hu & Kerppola, 2003), and its applications were later extended to investigate the self-assembly of amyloid-forming peptides and proteins (Outeiro et al., 2008).

The α-syn-BiFC system has been used to develop cellular assays to investigate several aspects of α-syn aggregation and biology, including 1) investigating the molecular and sequence determinants of α-syn oligomerization and aggregation (Aelvoet et al., 2014; Bae et al., 2014; K M Danzer et al., 2011; Karin M. Danzer et al., 2012; Delenclos et al., 2016; Gonçalves et al., 2016; Putcha et al., 2010; Savolainen et al., 2015; Tetzlaff et al., 2008; Zheng et al., 2018); 2) α-syn cell-to-cell transmission and propagation in cells and *C. elegans* (Kim et al., 2016); 3) the screening of genetic (Dettmer et al., 2015; Lázaro et al., 2016, 2014) and pharmacological modifiers (Dominguez-Meijide et al., 2020; Mohammadiet al., 2017; Moussaud et al., 2015) of α-syn oligomerization, aggregation and clearance; and 4) the validation of therapeutic targets (Outeiro et al., 2008). This approach was also extended to animal models of synucleinopathies, such as rats (Dimant et al., 2013), *C. elegans* (Kim et al., 2016) and, most recently, *Drosophila* (Prasad et al., 2018) and mice (Cai et al., 2018) (Kiechle et al., 2019).

While reviewing the literature, we noted the lack of data on 1) the biochemical validation of this system, i.e., evidence that it indeed reports on the formation of α-syn dimers, oligomers or higher-order aggregates; 2) the stability and oligomerization properties of the BiFC fragments; 3) whether the fluorescent signal arises only from the interaction between α-syn monomers or between monomers of one fragment and oligomers or aggregates of the other fragment (Figure 1C); and 3) the biochemical, structural or morphological properties of the

oligomers/aggregates that form upon co-expression of the BiFC fragments and to what extent they are similar or different from α-syn aggregates found in diseased brains or formed during the fibrillization of recombinant α-syn *in vitro*. To address this knowledge gap, we performed a more in-depth characterization of the α-syn-Venus BiFC system in HEK-293 cells using a combination of biochemical and cellular assays. Our results show that differential expression of the fluorescent protein fragments and their propensity self-associate on their own complicate the interpretation of the fluorescence signal in this BiFC cellular assay. These observations highlight the limitations of this system to investigate mechanisms and modifiers of α-syn oligomerization and inclusion formation. They also underscore the critical importance of the validation of BiFC-based assays at the biochemical and ultrastructural levels. This is crucial to determine if they indeed accurately reproduce and report on the process of interest, e.g., oligomerization, prior to their use to investigate mechanisms of protein oligomerization, amyloid formation or cell-to-cell transmission or to screen for modifiers of these processes.

Materials and Methods

Supporting Information

Antibodies

Antibody name	Company	Cat#	RRID	Dilution Used in Experiment
Syn-1	BD Biosciences	610787	AB_398108	Immunoblotting (1:1000) Immunocytochemistry (1:500)
GAPDH	Cell Signaling Technology	610787	AB_398108	Immunoblotting (1:1000)
beta-tubulin	Abcam	ab6046	AB_2210370	Immunoblotting (1:1000)
DJ-1	Abcam	ab18257	AB_444361	Immunoblotting (1:1000)
Rabbit IgG Alexa Fluor 680	Thermo Fisher Scientific	A32734	AB_2633283	Immunoblotting (1:5000)
Mouse IgG Alexa Fluor 800	Thermo Fisher Scientific	A32730	AB_2633279	Immunoblotting (1:5000)
Mouse Alexa Fluor 647	Thermo Fisher Scientific	A-31571	AB_162542	Immunocytochemistry (1:800)

Plasmids

The plasmid encoding WT-α-syn was cloned into a pAAV vector under the control of a CMV promoter in our laboratory (Addgene plasmid #36055; http://n2t.net/addgene:36055; RRID: Addgene36055). The Vn-α-syn (Addgene plasmid #89470; http://n2t.net/addgene:89470; RRID:Addgene_89470) and α-syn-Vc (Addgene plasmid # 89471; http://n2t.net/addgene:89471; RRID:Addgene_89471) plasmid fragments were both previously cloned into the backbone of pcDNA3.1 under the control of a CMV promoter and were a kind gift of Tiago Outeiro. The α-syn-Venus (α-syn-V) construct encoding α-syn fused to full-length Venus under the control of a CMV promoter in a pcDNA 3.1 backbone was a kind gift from Pamela McLean. Further details about each vector and the full sequences can be obtained upon request.

Cell culture and transfection protocol

HEK-293 cells were maintained in Dulbecco's modified Eagle medium (DMEM; Gibco, Cat# 31966-021) containing 10% FBS and streptomycin and penicillin (10 µg/ml) at 37 °C. Cells were transfected by the addition of polyethylenimine (PEI) (Polysciences Inc, Cat# 23966) to plasmid DNA in Opti-MEM (Gibco, # 31985-062) at a ratio of 1:3 (µg vector DNA:µg PEI). The added transfection mixture volume was 10% of the total volume of the cell culture medium present in each well. The amount of plasmid DNA used for transfection was 2 µg for 6-well plates and 10 µg for 10 cm dishes. For BiFC co-expression (Vn-α-syn and α-syn-Vc), 1 µg of each BiFC vector was used for 6-well plates, and 5 µg of each vector was used for 10 cm dishes.

Immunocytochemistry

HEK-293 cells (300 000 cells per well in 2 ml cell medium) were seeded onto coverslips coated with poly-L-lysine (Cultrex, Cat# 3438-100-01) and transfected as described above. Cells were washed 2 times with PBS and fixed in 3.7% formaldehyde (Sigma Aldrich) at RT for 15 min. Cells were then blocked and permeabilized simultaneously in PBS containing 3% BSA and 0,1% Triton X-100 (PBS-T) at RT for 30 min. α-syn was targeted by using the Syn-1 antibody (BD Biosciences) in PBS-T (diluted 1:500) at RT for 2 h. Cells were then rinsed five times with PBS-T and incubated with a cocktail of donkey anti-mouse Alexa Fluor 647 (1:800), DAPI (1:1500) and phalloidin-Atto 565 (1:150) (Sigma Aldrich, Cat# 94072) in PBS-T at RT for 1 h. Cells were then washed 4 times in PBS-T and finally rinsed with pure water before being mounted in polyvinyl alcohol (PVA) mounting medium with DABCO (Sigma Aldrich, Cat# 10981). Cells were then examined with a confocal laser scanning microscope using a 40x oil objective and Zen software (LSM 700, Zeiss).

Cell lysis

HEK-293 cells were plated in 6-well plates (300 000 cells per well in 2 ml cell medium) and lysed in RIPA buffer (150 mM NaCl, 50 mM Tris pH 8.0, 1% NP-40, 0.5% deoxycholate, and 0.1% SDS) supplemented with 1% protease cocktail inhibitor (Sigma Aldrich, Cat# PB8340) and 1% phenylmethylsulfonyl fluoride (Axon Lab, Cat# A0999.0005) 48 h after transfection. The cell suspension was then gently mixed while being rotated at 4 °C for 30 min, and the cell debris was pelleted afterwards by centrifugation at 4 °C and 13 000 g for 20 min. The supernatant fraction was then used for immunoblotting.

For analysis of the SDS-insoluble fractions, the samples were centrifuged for 30 min at 13 000 g instead of 20 min, and the insoluble fraction (pellet) was resuspended in TBS/SDS buffer (150 mM NaCl, 50 mM Tris, pH 7.5, and 2% SDS) and sonicated using a probe for 15 s (1 s on pulse/1 s off pulse) at a 20% amplitude. The soluble and insoluble fractions were then processed as described in the immunoblotting section.

Immunoblotting procedure

The total protein concentration for each sample was determined by the bicinchoninic acid assay (BCA, Thermo Scientific, Cat# 23225). Samples were next mixed (4:1) with 4X Laemmli buffer (2% sodium dodecyl sulfate (SDS), 20% glycerol, 0.05% bromophenol blue, 0.125 M Tris-HCl pH 6.8 and 5% β-mercaptoethanol). Samples were not boiled to maintain the stability of the protein interactions. Total cell lysates (10 µg) were separated with 15% SDS-PAGE (polyacrylamide gel electrophoresis) and transferred to a nitrocellulose membrane (Chemie Braunschweig, Cat# MSNC02030301) with a semidry system (BioRad, Cat# 1704150) at a constant amperage of 0.5 A and 25 V for 45 min. The membranes were then blocked with Odyssey Blocking buffer (Li-Cor, Cat# 927-40000) that was diluted 1:3 in PBS at 4 °C overnight. The membranes were then probed with the respective primary antibody (1:1000 diluted in PBS) on a shaking platform at RT for 2 h and then washed 3 times for 10 min in PBS-T (PBS, 0.1% Tween 20). The membranes were next incubated with the respective Alexa-conjugated secondary antibodies (goat anti-mouse IgG Alexa Fluor 800 or goat anti-rabbit IgG Alexa Fluor 680; 1:5000 in PBS) on a shaking platform while protected from light at RT for 1 h. The blots were finally washed 3 times in PBS-T and scanned by an Odyssey CLx Imaging System (Li-Cor Biosciences) at a wavelength of 700 or 800 nm.

Crosslinking of intact cultured cells

Cells cultured in 6-well plates (300 000 cells in 2 ml medium) were removed from the plate by enzymatic digestion via trypsinization 48 h post-transfection and collected by centrifugation of the cells at 300 g and RT for 3 min. Subsequently, the cells were resuspended in 600 µl of PBS containing protease inhibitors (Roche, Cat# 05892791001) and split into two 300 µl aliquots, of which one aliquot was treated with DSG (disuccinimidyl glutarate) crosslinker (1 mM) (Thermo Scientific, Cat# 20593), while the other served as a negative control, to which only DMSO was added. DSG was stored at 4 °C with desiccant and prepared fresh directly

before use by dissolving it in DMSO to make a 100 mM solution (100x stock solution). Crosslinking was performed under shaking conditions at 750 rpm for 30 min at 37 °C. The reaction was then quenched by adding Tris (50 mM, pH 7.6) and incubating it at RT for 15 min. Next, the cells were lysed by sonication (amplitude of 40%, 2 x 15 s) and centrifuged at 20 000 g for 30 min at 4 °C. The supernatant was collected, and the total protein concentration was determined by BCA; the sample was then mixed 1:1 with NuPAGE LDS sample buffer (Thermo Scientific, Cat# NP0007) and boiled at 95 °C for 10 min. Twenty micrograms of each sample was loaded on NuPAGE 4–12% Bis-Tris gels (Thermo Scientific, Cat# NP0322PK2) with NuPAGE MES-SDS running buffer (Thermo Scientific, Cat# NP0002). After electrophoresis, the proteins were electroblotted onto PVDF membranes (Millipore, ISEQ00010), which were further processed as described in the immunoblotting section.

Size exclusion chromatography

Cells were plated in 10 cm dishes (2,2 x 10^6 cells) and transfected as previously described. Cells were lysed 48 h post-transfection by nonionic detergent lysis buffer (20 mM Tris pH 7.4, 150 mM NaCl, 1 mM EDTA, 0.25% NP40, and 0.25% Triton X-100) supplemented with 1% protease cocktail inhibitor (Sigma Aldrich, Cat# PB340) and 1% phenylmethylsulfonyl fluoride (Axon Lab, Cat# A0999.0005) under gentle rotation for 30 min at 4 °C. Cell lysates were then cleared by centrifugation at 13 000 g for 30 min at 4 °C, and 300 µl of the collected supernatant was directly injected into a Superdex 200 HR 10/300 column (GE Healthcare Life Science, Cat# 17517501). To avoid any aggregation artefacts due to freezing and thawing of the samples, the cell lysates were directly subjected to size exclusion chromatography using an ÄKTA purifier (GE Healthcare Life Science). The column was washed with three column volumes (75 ml) of Milli-Q and equilibrated with three column volumes of filtered PBS (20 mM sodium phosphate, 150 mM NaCl, pH 7.4) at a flow rate of 0.3 ml/min. An injection loop with a 500 µl volume was used to introduce the analytes and washed with 5 ml of buffer manually using a plastic syringe before each run. The flow rate for each run was set to 0.5 ml/min at 4 °C, and the collection volume was set to 500 µl. From each size fraction, a 40 µl aliquot was directly mixed with 10 µl of 4x Laemmli buffer (2% sodium dodecyl sulfate (SDS), 20% glycerol, 0.05% bromophenol blue, 0.125 M Tris-HCl, pH 6.8 and 5% β-mercaptoethanol), and each sample was then subjected to immunoblotting as described in the corresponding section. For calibration, the Superdex 200 column was calibrated using a gel filtration HMW calibration kit

(GE Healthcare Life Science, Cat# 28403842) that included six reference proteins with known molecular weights (MWs) (ranging from 43-669 kDa). The standard curve generated allowed us to calculate the apparent MW of each eluted α-syn construct (Fig. 4C). Dextran blue 2000 produced a peak at 7,78 ml, which defined the void volume (V_o) and thereby the maximal size of the proteins that could be separated (Fig. 4B).

Results

The two α-syn-Venus BiFC fragments were expressed in HEK-293 cells at drastically different levels

As a first step in characterizing the Venus-α-syn BiFC system, we sought to assess the expression levels and stability of the individual fragments and the full-length α-syn fused to full-length Venus (α-syn-Venus). The constructs corresponding to these proteins were overexpressed in HEK-293 cells, and the cell lysates were analyzed by Western blotting (WB) with antibodies against α-syn as well as the N- and C-terminal fragments of Venus (abbreviated as Vn-α-syn and α-syn-Vc, respectively). As shown in Fig. 3A, both the full-length α-syn-Venus and Vn-α-syn proteins were expressed at high levels, whereas the band corresponding to α-syn-Vc was barely detectable in comparison to that of Vn-α-syn (Fig. 3A). When expressed individually, Vn-α-syn was expressed at 6- to 16-fold higher levels than α-syn-Vc (Fig. 3A) and at levels higher than those of any of the other tested constructs (WT-α-syn, α-syn-Vc and α-syn-Venus), suggesting the increased stability or decreased turnover of Vn-α-syn, which was consistent with previous observations (Dominguez-Meijide et al., 2020; Eckermann, Kügler, & Bähr, 2015; Lázaro et al., 2014).

When the two constructs were co-expressed, the α-syn-Vc protein band disappeared, while a new band corresponding to the Vn-α-syn + Vc-α-syn dimer was detected. This is consistent with previous reports of the irreversible dimerization of these proteins upon successful reconstitution by BiFC (Hu et al., 2002). However, the band intensity of Vn-α-syn remained at a level that is comparable to that observed when the protein was expressed alone. These results suggest that only a small fraction of Vn-α-syn associates with α-syn-Vc and is involved in the formation of the fluorescent BiFC complex.

To assess whether it would be possible to increase the levels of α-syn-Vc and achieve an equimolar concentration of both BiFC constituents, we varied the amounts of vector DNA applied for transfection. The protein level of WT-α-syn increased with the amount of vector DNA used for transfection (Fig. 3C). Strikingly, despite the transfection of six times more α-syn-Vc than Vn-α-syn, the levels of α-syn-Vc remained unchanged (Fig. 3C-D). Surprisingly, this imbalance was repeatedly observed but not discussed in previous studies (Cai et al., 2018; Dominguez-Meijide et al., 2020; Eckermann et al., 2015a; Lázaro et al., 2016, 2014; Prasad et al., 2018; Zondler et al., 2014). Only one report (Eckermann et al., 2015) suggested that the differential expression of the two constructs could lead to a potential entrapment of α-syn-Vc by the strongly overexpressed Vn-α-syn to force the less abundantly expressed protein into an non-specific interaction.

Vn-α-syn exhibits a high propensity to form oligomers and higher-order aggregates

Next, we sought to investigate the biochemical and oligomerization properties of each of the BiFC fragments. Towards this end, the lysates of HEK-293 cells expressing the various α-syn BiFC proteins were size-separated by size exclusion chromatography (SEC). To assess whether any of the reagents or the process of cell lysis affected the size separation, the elution pattern of recombinant α-syn (Fig. 4B, gray line) was compared to that of the lysate of WT-α-syn-expressing HEK-293 cells (Fig. 4B, orange line). α-syn eluted at 13-14 ml for both samples, suggesting that intracellular α-syn exists predominantly as a monomer, which is consistent with previous findings by our group (Fauvet et al., 2012) and others (Weinreb, Zhen, Poon, Conway, & Lansbury, 1996).

The largest α-syn construct, α-syn-Venus (Fig. 4B, green), eluted from 8 to 14,5 ml, with the most intense band detected at 11-13 ml, suggesting that α-syn-Venus has a low propensity to form higher-order oligomers and that the majority of the protein exists in monomeric forms. Given that Vn-α-syn and α-syn-Vc have sizes that are intermediate between those of α-syn-V and WT-α-syn, we expected these proteins to elute at volumes between 8 ml and ~14 ml. As expected, α-syn-Vc (Fig. 4B, blue) eluted at 13 ml, but in contrast (Fig. 4B, red), the majority of Vn-α-syn eluted at the void volume of 7,5 ml, indicative of the high propensity of this protein to self-oligomerize. When both BiFC constructs were co-expressed (Fig. 4B, yellow), the band corresponding to the size of Vn-α-syn still eluted mainly at the void volume. Interestingly, α-syn-Vc was now detected in higher MW fractions (10 ml), possibly due to a

shift caused by the dimerization of the BiFC constructs, which is consistent with what we observed by WB (Fig. 3A). Furthermore, the detection of the band corresponding to the BiFC-α-syn dimer complex in the void volume suggested that this complex goes on to form higher-order oligomers or that it is sequestered by the aggregates formed by the Vn-α-syn fragment (Eckermann et al., 2015).

Crosslinking studies confirm that Vn-α-syn but not α-syn-Vc forms higher MW weight oligomers

To further characterize the aggregation propensities of the various α-syn BiFC fragments, we performed intact cell crosslinking and assessed the oligomerization by WB. DJ-1, which forms dimers in physiological conditions, was used as a positive control (Dettmer et al., 2015). The crosslinked cell lysate displayed DJ-1 dimer bands that were absent in non-crosslinked cells, indicating the success of crosslinking at the concentration of the DSG crosslinker used in our experiments (Fig. 5C). WT α-syn was mainly detected as a monomer (15 kDa), but a noticeable stochastic ladder of monomers, dimers, trimers and so on up to the stacking gel was also observed (Fig. 5B). α-syn-Venus displayed two monomeric bands: one at the expected size of 42 kDa and one band at the lower size of approximately 36 kDa, which we observed whenever we did not boil the samples prior to immunoblotting and probably represents a more compact folded structure of this fusion protein. In concordance with the SEC results, α-syn-Vc showed a single band at the expected MW, and no higher MW species were detectable. In contrast, Vn-α-syn formed several higher MW bands, including a prominent band that remained in the stacking gel. These high molecular weight (HMW) aggregates were only observed when intact cell crosslinking was performed. This suggests that in the absence of crosslinking, the majority of the Vn-α-syn oligomers are SDS-sensitive and break down into monomers in denaturing conditions. Upon co-expression, the Vn-α-syn/α-syn-Vc dimer band intensity increased, while the intensity of the individual monomeric bands was reduced. Additionally, as a result of co-expression, the stacking gel showed an α-syn signal, indicating the presence of high-molecular-weight α-syn species, although the intensity of the corresponding band was weaker than that representing the expression of Vn-α-syn alone. The the aggregation seen here is likely driven by Vn-α-syn, as α-syn-Vc alone did not produce any higher MW aggregates. Together, the results from the crosslinking and SEC experiments demonstrated that Vn-α-syn exhibits a high propensity to self-oligomerize and exists predominantly in oligomeric forms.

Vn-α-syn predominantly forms soluble SDS-sensitive oligomers in cells

To determine whether the BiFC fragments form oligomers or higher-order aggregates such as fibrils, the lysates from HEK-293 cells expressing the different proteins were separated by centrifugation into soluble and insoluble fractions (Fig. 6A). Consistent with the data presented above, WB analyses showed that Vn-α-syn was predominantly detected in the soluble fraction. This suggests that it self-assembles into soluble oligomers, which also eluted in the volume peak of the SEC column (Fig. 4B) but disassociated into monomers in the presence of SDS (Fig. 6B). The Vn-α-syn fragment was also detected in the insoluble fractions, suggesting that small fraction of this fragment goes on to form insoluble aggregates. In contrast, none of the other constructs, including α-syn-Vc, was detected in the insoluble fractions. Interestingly, when the two BiFC fragments were co-expressed, only Vn-α-syn was efficiently enriched in the insoluble fraction. Traces of α-syn-Vc and the BiFC complexes could be detected in this sample, which could be due to the fact that these species become entrapped within or non-specifically interact with the Vn-α-syn aggregates.

Neither of the BiFC fragments when expressed alone or when co-expressed in cells form α-synuclein amyloid-like aggregates or inclusions

Finally, we sought to characterize the aggregation properties of the BiFC fragments in intact cells by immunocytochemistry. The proteins were expressed in HEK-293 cells, and their localization and aggregation were assessed using an α-syn specific antibody (Syn-1). We used α-syn-Venus as a positive control, as full-length Venus is expected to emit fluorescence, and untagged α-syn as a negative control. As expected, no Venus fluorescence was observed when the individual BiFC fragments, Vn-α-syn or α-syn-Vc, were expressed on their own, while co-expression of both proteins led to intense signals from Venus as a result of complementation (Fig. 7). Fluorescence was observed both in the cytosol and the nucleus, as previously reported (Dettmer et al., 2015; Lázaro et al., 2016, 2014; Moussaud et al., 2015). We did not observe the formation of foci or inclusions for any of the BiFC constructs used in our conditions, which is consistent with the results from the biochemical and SEC studies, which showed that the BiFC fragments, either alone or when co-expressed, mainly formed soluble oligomers. To specifically assess the presence of amyloid-like aggregates, we treated the cells with the amyloid-specific dye Amytracker (Mahul-Mellier et al., 2020). We did not observe any

Amytracker-positive structures in cells regardless of which construct(s) were expressed (data not shown). These observations demonstrate the absence of insoluble aggregated or fibrillar forms of α-syn, suggesting that the oligomers formed by the Venus BiFC fragments or BiFC fluorescent complex do not go on to form fibril and may not share properties with oligomers that form on the pathway to α-syn fibril formation. Further studies are needed to characterize the biochemical and structural properties of the α-syn oligomers formed by the BiFC fragments to determine to what extent they resemble native α-syn oligomers.

Discussion

Several α-syn BiFC cellular assays (Gonçalves et al., 2010) have been developed and are increasingly used in cellular and animal studies aimed at investigating the mechanisms of α-syn aggregation, propagation and toxicity and target identification and validation or screening and evaluating genetic, enzymatic and pharmacological modulators of α-syn aggregation, toxicity and clearance (Cai et al., 2018; Dimant et al., 2013; Eastwood et al., 2017; Moussaud et al., 2015; Outeiro et al., 2008; Prasad et al., 2018) (Kiechle et al., 2019). Despite this, there has been very little effort to validate these assays (Eckermann et al., 2015) at the biochemical level and to characterize the nature of the α-syn oligomers that form upon reconstitution of the α-syn BiFC fragments and fluorescence signal. The primary objectives of this study was to contribute to addressing this knowledge gap by 1) providing insight into the molecular interactions that give rise to the fluorescence signal observed in these assays; and 3) investigating the solubility and aggregation state of the α-syn BiFC fragments and complexes.

Our study showed that α-syn-Vc is expressed in minute amounts and that only a fraction of Vn-α-syn participates in the formation of complexes that give rise to the fluorescence signal. This large difference in protein expression levels between the two fragments has been consistently observed in previous studies but has rarely been discussed (Bartels et al., 2019) (Delenclos et al., 2019) (Cai et al., 2018; Eckermann et al., 2015; Gonçalves et al., 2016; Herrera & Outeiro, 2012; Lázaro et al., 2016, 2014; Moussaud et al., 2015; Prasad et al., 2018; Zondler et al., 2014). Interestingly, even when the Venus-BiFC fragments were expressed in Drosophila, the α-syn-Vc fragment protein was expressed at significantly lower levels compared to the Vn-α-syn fragment (Prasad et al., 2018). Despite this observation, the

authors in this study chose to quantify the levels of insoluble α-syn protein levels using a filter retardation assay, which does not allow for the determination of the nature and distribution of the α-syn species in the insoluble fractions, i.e., if the aggregates consist purely of the aggregation-prone fragment Vn-α-syn or Vn-α-syn together with the α-syn-Vc fluorescent complex. In a recent study, Kiechle et al developed two transgenic mouse models using two protein complementation systems, where α-syn was fused to N- or C-terminal part of hGaussia Luciferase or YFP Venus halves, to investigate age-dependent changes in α-syn oligomerization and aggregation at the synapse (Kiechle et al., 2019). For the hGaussia Luciferase protein-fragment system, the two fragments were expressed at different levels with one fragment expressing at much higher levels compared to the other fragment. For the Venus system, author present data that shows both equal expression of the two BiFC fragments and also data that show differential expression and significantly reduced levels of α-syn-Vc, consistent with our findings.

A possible explanation for the difference in protein levels might be the arrangement of the BiFC fusion proteins (Fig. 2), as the split Venus fragments were fused at the opposite ends of α-syn, which may influence α-syn stability or clearance. Interestingly, such differences in protein expression levels have been consistently observed in the cases of the cellular assays of the fusions of Venus-BiFC with α-syn, amyloid precursor protein (AβPP) (So et al., 2013) and exon1 of the huntingtin protein (Httex1) (Herrera et al., 2011) but not the Luciferase- or GFP-based BiFC systems, where both complementation constituents were fused to the carboxy-terminus of α-syn and showed comparable protein levels (Mohammadi et al., 2017; Moussaud et al., 2015; Outeiro et al., 2008) and half-lives (Moussaud et al., 2015). The large differences in the protein levels of the two Venus BiFC fragments combined with the high aggregation propensity of Vn-α-syn highlight the critical importance of assessing the expression and aggregation state of each component of the Venus BiFC systems and other BiFC systems to ensure accurate interpretation of experimental findings. In the absence of such insight, it is difficult to correlate the differences in the fluorescence signal to the propensity of α-syn to oligomerize or speculate about the mechanisms of α-syn oligomerization, aggregation and toxicity in these cellular assays. This is especially important when the fluorescence signal arises from only a small fraction of the total α-syn expressed in the cell. Finally, whether the oligomers formed by Vn-α-syn could influence α-syn cellular properties in cellular assays using

Venus-BiFC system remains unknown (Kiechle et al., 2019; Zondler et al., 2014). Together, these observations underscore the limitations of relying solely on the fluorescence signal as the primary readout of α-syn oligomerization.

Although previous studies did not thoroughly investigate the oligomerization properties of the individual BiFC fragments, two studies showed, by using denaturing (Roberts et al., 2015) and native gel electrophoresis (Outeiro et al., 2008; Roberts et al., 2015), that some GFP-BiFC fragments has the propensity to form high molecular weight oligomers on its own (Kerppola, 2008). Despite the fact that in both studies and in a previous report (Magliery et al., 2005), the fragment with GFP/Venus fused to the N-terminus of α-syn exhibited increased oligomer formation, the significance and implications of these observations were not discussed or accounted for in the interpretation of the results. In another study by Dettmer and colleagues, intact cell crosslinking followed by WB analysis showed the presence HMW species corresponding to Vn-α-syn only, which is again consistent with our findings (Dettmer et al., 2015). Furthermore, Bae et al showed that only Vn-α-syn was secreted by cells and existed as a mixture of monomers and aggregates in the cell culture medium (Bae et al., 2014), consistent with our data (Fig. 4A). When the cell culture media containing Vn-α-syn monomers and aggregates were added to cells stably expressing α-syn-Vc, fluorescent foci were observed in the host cells. If the Vn-α-syn aggregates were removed prior to addition to other host cells, no BiFC signal was observed. These observations suggest that the fluorescence signal observed in the host cell arise due to the recruitment and/or entrapment of the α-syn-Vc monomers in the preformed Vn-α-syn aggregates rather than interactions between the two monomers, which is consistent with our observations and those of previous reports (Eckermann et al., 2015). This experiment illustrates the challenges in interpreting BiFC fluorescence signal in systems where different BiFC fragments exhibit differences in protein levels, biophysical properties and aggregation propensity and demonstrate that other aberrant interactions, in addition to the expected multimerization may give rise to the BiFC fluorescence signal.

One way to validate the BiFC-based oligomerization cellular assays is to assess the specificity of the interactions by using mutant forms of the protein of interest that exhibit no or a very low propensity to self-associate or by using closely related proteins that are known to not

interact with one another or to self-oligomerize (Hu et al., 2002; Kudla & Bock, 2016). In these cases, one would expect no or very little fluorescent signal when compared to that of BiFC protein partners that indeed oligomerize. Indeed, this approach has already been applied by several groups to investigate the utility of the Venus BiFC system to compare the oligomerization properties of the different members of the α-syn family (Eckermann et al., 2015) and various α-syn disease-associated mutants (Dettmer et al., 2015; Lázaro et al., 2016, 2014). For example, Eckermann and colleagues reported no detectable differences in the Venus BiFC signal when α-, β- and ɣ-syn oligomerization were assessed in parallel, suggesting that they exhibit similar homodimerization properties (Eckermann et al., 2015). This is surprising, as β-syn is known to not aggregate, does not form inclusions in cells or in the brain and has consistently been shown not to form fibrils under physiological conditions (Ghosh et al., 2015). Similarly, one would expect an increased BiFC signal when using proteins with disease-specific point mutations that promote α-syn aggregation, such as the A53T mutation. Although several α-syn PD-associated mutants have been shown to promote α-syn oligomerization and/or fibril formation *in vitro* (de Oliveira & Silva, 2019; Ruf et al., 2019), in cells (M. B. Fares et al., 2014; Khalaf et al., 2014; Lei, et al., 2019) and *in vivo* (Mbefo et al., 2015; Paumier et al., 2013), Lázaro et al. reported identical Venus BiFC signals from WT α-syn and the PD-linked mutants A30P, E46K, H50Q, G51D and A53T (Lázaro et al., 2014). Similar observation were made by Outeiro et al using a GFP-BiFC cellular assay (Outeiro et al., 2008). It was suggested that these observations could be explained by the possibility that the dimerization propensity of the α-syn proteins to form dimers does not reflect their oligomerization and aggregation properties (Eckermann et al., 2015). However, this interpretation is not consistent with extensive biophysical studies using different approaches that have shown significant differences in the propensity of α-syn the various PD-linked α-syn mutants to form oligomers (Winner et al., 2011) and dimers (Janowskaet al., 2015; Lv et al., 2016). In addition, several studies have shown significant differences in the lifetime and distribution of different types of dimers formed by wild-type α-syn and PD-linked mutants (Krasnoslobodtsev et al., 2013; Krishnan et al., 2003; Lv et al., 2015). Taken together, these results demonstrate that the current α-syn BiFC cellular assays are not predictive of the propensity of α-syn to form oligomers or fibrils.

Despite these limitations, several studies have demonstrated that the α-syn BiFC system could be useful to investigate α-syn cell-to-cell transmission (Bae et al., 2014; K. M. Danzer et al., 2011; Kim et al., 2016; Wang et al., 2014). In these experiments, each BiFC fragment is expressed in different cells which are then co-cultured and α-syn cell-to-cell transfer is monitored by the reconstitution of the BiFC fluorescence signal in either cell. In such studies, it is still crucial to biochemically assess the aggregation state of the BiFC fragment that is formed and secreted by each cell lines. These recommendations are in line with those made previously by Eckermann et al (Eckermann et al., 2015).

Conclusions

The design of BiFC systems to investigate protein-protein interactions or protein self-assembly is based on three assumptions: 1) the individual reporter fragments do not self-associate unless the proteins they are fused to interact with each other or have the propensity to dimerize or oligomerize (Kerppola, 2006); 2) both BiFC fragments are expressed at equal levels; and 3) mutants that disrupt or enhance protein-protein interactions should result in a decrease or an increase in the fluorescence signal, respectively. While our studies confirm that a fluorescence signal is observed only when both BiFC fragments fused to α-syn are co-expressed in the cell, they also clearly demonstrate that 1) the two BiFC fragments, Vn-α-syn and α-syn-Vc, are not expressed at equal levels; 2) the Vn-α-syn fragment exhibits a high propensity to aggregate; and 3) the fluorescence signal observed may not arise only from α-syn dimerization and could also be derived from the association or entrapment of α-syn-Vc in the Vn-α-syn aggregates. Together, these observations combined with previous findings of independent groups demonstrate that the α-syn-Venus-BiFC system does not reveal known differences in the oligomerization and aggregation propensities of PD-associated variants or the interactions between mutants and WT α-syn (Eckermann et al., 2015). Finally, consistent with previous reports, we showed that overexpression of either Vn-α-syn or the two BiFC fragments results in the formation of α-syn oligomers that do not seem to convert to inclusions or amyloid-like aggregates (Dettmer et al., 2015b; Gonçalves et al., 2016; Kiechle et al., 2019; Lázaro et al., 2014; Moussaud et al., 2015; Outeiro et al., 2008). Together, these findings underscore the critical importance of characterizing BiFC-based cellular assays at the biochemical and structural levels and understanding how the fusion of fragments of

fluorescent proteins influences α-syn biophysical and cellular properties before using such assays in mechanistic, target validation and drug discovery studies.

Acknowledgments

This work was supported by funding from EPFL. We are grateful to the Bioimaging Core Facility (BioP, EPFL) for their technical support. We would also like to thank Dr. Senthil Kumar for his technical help with size exclusion chromatography, Muhammed Syed for providing some of the recombinant proteins used as standards and in the SEC studies. Dr. Anne-Laure Mahul and Nathan Riguet for helpful discussions and Dr. Kolla Rajasekhar for generating the graphical abstract. We would also like to thank Prof. Tiago Outeiro and Prof. Pamela McLean for providing us with the α-syn-Venus-BiFC expression vectors used in this study.

References

Aelvoet, S.-A., Ibrahimi, A., Macchi, F., Gijsbers, R., Van den Haute, C., Debyser, Z., & Baekelandt, V. (2014). Noninvasive Bioluminescence Imaging of α-Synuclein Oligomerization in Mouse Brain Using Split Firefly Luciferase Reporters. *The Journal of Neuroscience*, *34*(49), 16518–16532. https://doi.org/10.1523/JNEUROSCI.4933-13.2014

Bae, E. J., Yang, N. Y., Song, M., Lee, C. S., Lee, J. S., Jung, B. C., … Lee, S. J. (2014). Glucocerebrosidase depletion enhances cell-to-cell transmission of α-synuclein. *Nature Communications*, *5*. https://doi.org/10.1038/ncomms5755

Bartels, M., Weckbecker, D., Kuhn, P. H., Ryazanov, S., Leonov, A., Griesinger, C., … Giese, A. (2019). Iron-mediated aggregation and toxicity in a novel neuronal cell culture model with inducible alpha-synuclein expression. *Scientific Reports*, *9*(1), 1–13. https://doi.org/10.1038/s41598-019-45298-6

Cai, W., Feng, D., Schwarzschild, M. A., McLean, P. J., & Chen, X. (2018). Bimolecular Fluorescence Complementation of Alpha-synuclein Demonstrates its Oligomerization with Dopaminergic Phenotype in Mice. *EBioMedicine*, *29*, 13–22. https://doi.org/10.1016/j.ebiom.2018.01.035

Danzer, K. M., Ruf, W. P., Putcha, P., Joyner, D., Hashimoto, T., Glabe, C., … McLean, P. J. (2011). Heat-shock protein 70 modulates toxic extracellular -synuclein oligomers and rescues trans-synaptic toxicity. *The FASEB Journal*, *25*(1), 326–336. https://doi.org/10.1096/fj.10-164624

Danzer, Karin M., Kranich, L. R., Ruf, W. P., Cagsal-Getkin, O., Winslow, A. R., Zhu, L., … McLean, P. J. (2012). Exosomal cell-to-cell transmission of alpha synuclein oligomers. *Molecular Neurodegeneration*, *7*(1), 1–18. https://doi.org/10.1186/1750-1326-7-42

de Oliveira, G. A. P., & Silva, J. L. (2019). Alpha-synuclein stepwise aggregation reveals features of an early onset mutation in Parkinson's disease. *Communications Biology*, *2*(1). https://doi.org/10.1038/s42003-019-0598-9

Delenclos, M., Burgess, J. D., Lamprokostopoulou, A., Outeiro, T. F., Vekrellis, K., & McLean, P. J. (2019). Cellular models of alpha-synuclein toxicity and aggregation. *Journal of Neurochemistry*, *150*(5), 566–576. https://doi.org/10.1111/jnc.14806

Delenclos, M., Trendafilova, T., Jones, D. R., Moussaud, S., Baine, A. M., Yue, M., … McLean, P. J. (2016). A rapid, semi-quantitative assay to screen for modulators of Alpha-synuclein oligomerization ex vivo. *Frontiers in Neuroscience*, *9*(JAN), 1–11. https://doi.org/10.3389/fnins.2015.00511

Dettmer, U., Newman, A. J., Soldner, F., Luth, E. S., Kim, N. C., Von Saucken, V. E., … Selkoe, D. (2015). Parkinson-causing α-synuclein missense mutations shift native tetramers to monomers as a mechanism for disease initiation. *Nature Communications*, *6*, 1–15. https://doi.org/10.1038/ncomms8314

Dimant, H., Kalia, S. K., Kalia, L. V, Zhu, L. N., Kibuuka, L., Ebrahimi-Fakhari, D., … McLean, P. J. (2013). Direct detection of α synuclein oligomers in vivo. *Acta Neuropathol Commun*, *1*, 6. https://doi.org/10.1186/2051-5960-1-6

Dominguez-Meijide, A., Vasili, E., König, A., Cima-Omori, M.-S., Leonov, A., Ryazanov, S., … Outeiro, T. F. (2020). Effects of pharmacological modulators of α-synuclein and tau aggregation and internalization. *BioRxiv*, 1–54.

Eastwood, T. A., Baker, K., Brooker, H. R., Frank, S., & Mulvihill, D. P. (2017). An enhanced recombinant amino-terminal acetylation system and novel in vivo high-throughput screen for molecules affecting α-synuclein oligomerisation. *FEBS Letters*, *591*(6), 833–841. https://doi.org/10.1002/1873-3468.12597

Eckermann, K., Kügler, S., & Bähr, M. (2015). Dimerization propensities of Synucleins are not

predictive for Synuclein aggregation. *Biochimica et Biophysica Acta - Molecular Basis of Disease*, *1852*(8), 1658–1664. https://doi.org/10.1016/j.bbadis.2015.05.002

Fares, M.-B., Maco, B., Oueslati, A., Rockenstein, E., Ninkina, N., Buchman, V. L., … Lashuel, H. A. (2016). Induction of de novo α-synuclein fibrillization in a neuronal model for Parkinson's disease. *Proceedings of the National Academy of Sciences*, *113*(7), E912–E921. https://doi.org/10.1073/pnas.1512876113

Fares, M. B., Ait-Bouziad, N., Dikiy, I., Mbefo, M. K., Jovičić, A., Kiely, A., … Lashuel, H. A. (2014). The novel Parkinson's disease linked mutation G51D attenuates in vitro aggregation and membrane binding of α-synuclein, and enhances its secretion and nuclear localization in cells. *Human Molecular Genetics*, *23*(17), 4491–4509. https://doi.org/10.1093/hmg/ddu165

Fauvet, B., Mbefo, M. K., Fares, M. B., Desobry, C., Michael, S., Ardah, M. T., … Lashuel, H. A. (2012). α-Synuclein in central nervous system and from erythrocytes, mammalian cells, and Escherichia coli exists predominantly as disordered monomer. *Journal of Biological Chemistry*, *287*(19), 15345–15364. https://doi.org/10.1074/jbc.M111.318949

Ghosh, D., Singh, P. K., Sahay, S., Jha, N. N., Jacob, R. S., Sen, S., … Maji, S. K. (2015). Structure based aggregation studies reveal the presence of helix-rich intermediate during α-Synuclein aggregation. *Scientific Reports*, *5*, 1–15. https://doi.org/10.1038/srep09228

Goedert, M., Jakes, R., & Spillantini, M. G. (2017). The Synucleinopathies: Twenty Years on. *Journal of Parkinson's Disease*, *7*(s1), S53–S71. https://doi.org/10.3233/JPD-179005

Gonçalves, S. A., Macedo, D., Raquel, H., Simões, P. D., Giorgini, F., Ramalho, J. S., … Outeiro, T. F. (2016). shRNA-Based Screen Identifies Endocytic Recycling Pathway Components That Act as Genetic Modifiers of Alpha-Synuclein Aggregation, Secretion and Toxicity. *PLoS Genetics*, *12*(4), 1–26. https://doi.org/10.1371/journal.pgen.1005995

Gonçalves, S. A., Matos, J. E., & Outeiro, T. F. (2010). Zooming into protein oligomerization in neurodegeneration using BiFC. *Trends in Biochemical Sciences*, *35*(11), 643–651. https://doi.org/10.1016/j.tibs.2010.05.007

Herrera, F., & Outeiro, T. F. (2012). α-Synuclein modifies huntingtin aggregation in living cells. *FEBS Letters*, *586*(1), 7–12. https://doi.org/10.1016/j.febslet.2011.11.019

Herrera, F., Tenreiro, S., Miller-Fleming, L., & Outeiro, T. F. (2011). Visualization of cell-to-cell transmission of mutant huntingtin oligomers. *PLoS Currents*. https://doi.org/10.1371/currents.RRN1210

Hu, C. D., Chinenov, Y., & Kerppola, T. K. (2002). Visualization of interactions among bZIP and Rel family proteins in living cells using bimolecular fluorescence complementation. *Molecular Cell*, *9*(4), 789–798. https://doi.org/10.1016/S1097-2765(02)00496-3

Hu, C. D., & Kerppola, T. K. (2003). Simultaneous visualization of multiple protein interactions in living cells using multicolor fluorescence complementation analysis. *Nature Biotechnology*, *21*(5), 539–545. https://doi.org/10.1038/nbt816

Janowska, M. K., Wu, K. P., & Baum, J. (2015). Unveiling transient protein-protein interactions that modulate inhibition of alpha-synuclein aggregation by beta-synuclein, a pre-synaptic protein that co-localizes with alpha-synuclein. *Scientific Reports*, *5*(October), 1–10. https://doi.org/10.1038/srep15164

Kerppola, T. K. (2006). Design and implementation of bimolecular fluorescence complementation (BiFC) assays for the visualization of protein interactions in living cells. *Nature Protocols*, *1*(3), 1278–1286. https://doi.org/10.1038/nprot.2006.201

Kerppola, T. K. (2008). Bimolecular Fluorescence Complementation (BiFC) Analysis as a Probe of Protein Interactions in Living Cells. *Annual Review of Biophysics*, *37*(1), 465–487.

https://doi.org/10.1146/annurev.biophys.37.032807.125842
Khalaf, O., Fauvet, B., Oueslati, A., Dikiy, I., Mahul-Mellier, A. L., Ruggeri, F. S., … Lashuel, H. A. (2014). The H50Q mutation enhances αα-synuclein aggregation, secretion, and toxicity. *Journal of Biological Chemistry*, *289*(32), 21856–21876. https://doi.org/10.1074/jbc.M114.553297
Kiechle, M., von Einem, B., Höfs, L., Voehringer, P., Grozdanov, V., Markx, D., … Danzer, K. M. (2019). In Vivo Protein Complementation Demonstrates Presynaptic α-Synuclein Oligomerization and Age-Dependent Accumulation of 8–16-mer Oligomer Species. *Cell Reports*, *29*(9), 2862-2874.e9. https://doi.org/10.1016/j.celrep.2019.10.089
Kim, D. K., Lim, H. S., Kawasaki, I., Shim, Y. H., Vaikath, N. N., El-Agnaf, O. M. A., … Lee, S. J. (2016). Anti-aging treatments slow propagation of synucleinopathy by restoring lysosomal function. *Autophagy*, *12*(10), 1849–1863. https://doi.org/10.1080/15548627.2016.1207014
Krasnoslobodtsev, A. V., Volkov, I. L., Asiago, J. M., Hindupur, J., Rochet, J. C., & Lyubchenko, Y. L. (2013). α-Synuclein misfolding assessed with single molecule AFM force spectroscopy: Effect of pathogenic mutations. *Biochemistry*, *52*(42), 7377–7386. https://doi.org/10.1021/bi401037z
Krishnan, S., Chi, E. Y., Wood, S. J., Kendrick, B. S., Li, C., Garzon-Rodriguez, W., … Carpenter, J. F. (2003). Oxidative dimer formation is the critical rate-limiting step for parkinson's disease α-synuclein fibrillogenesis. *Biochemistry*, *42*(3), 829–837. https://doi.org/10.1021/bi026528t
Kudla, J., & Bock, R. (2016). Lighting the Way to Protein-Protein Interactions: Recommendations on Best Practices for Bimolecular Fluorescence Complementation Analyses. *The Plant Cell*, *28*(5), 1002–1008. https://doi.org/10.1105/tpc.16.00043
Lashuel, H. A., Overk, C. R., Oueslati, A., & Masliah, E. (2012). The many faces of α-synuclein: from structure and toxicity to therapeutic target. *Nature Reviews Neuroscience*, *14*(1), 38–48. https://doi.org/10.1038/nrn3406
Lázaro, D. F., Dias, M. C., Carija, A., Navarro, S., Madaleno, C. S., Tenreiro, S., … Outeiro, T. F. (2016). The effects of the novel A53E alpha-synuclein mutation on its oligomerization and aggregation. *Acta Neuropathologica Communications*, *4*(1), 128. https://doi.org/10.1186/s40478-016-0402-8
Lázaro, D. F., Rodrigues, E. F., Langohr, R., Shahpasandzadeh, H., Ribeiro, T., Guerreiro, P., … Outeiro, T. F. (2014). Systematic Comparison of the Effects of Alpha-synuclein Mutations on Its Oligomerization and Aggregation. *PLoS Genetics*, *10*(11). https://doi.org/10.1371/journal.pgen.1004741
Lee, H. J., & Lee, S. J. (2002). Characterization of cytoplasmic α-synuclein aggregates. Fibril formation is tightly linked to the inclusion-forming process in cells. *Journal of Biological Chemistry*, *277*(50), 48976–48983. https://doi.org/10.1074/jbc.M208192200
Lei, Z., Cao, G., & Wei, G. (2019). A30P mutant α-synuclein impairs autophagic flux by inactivating JNK signaling to enhance ZKSCAN3 activity in midbrain dopaminergic neurons. *Cell Death and Disease*, *10*(2). https://doi.org/10.1038/s41419-019-1364-0
Lv, Z., Krasnoslobodtsev, A. V., Zhang, Y., Ysselstein, D., Rochet, J. C., Blanchard, S. C., & Lyubchenko, Y. L. (2015). Direct detection of α-synuclein dimerization dynamics: Single-molecule fluorescence analysis. *Biophysical Journal*, *108*(8), 2038–2047. https://doi.org/10.1016/j.bpj.2015.03.010
Lv, Z., Krasnoslobodtsev, A. V., Zhang, Y., Ysselstein, D., Rochet, J. C., Blanchard, S. C., & Lyubchenko, Y. L. (2016). Effect of acidic pH on the stability of α-synuclein dimers. *Biopolymers*, *105*(10), 715–724. https://doi.org/10.1002/bip.22874

Magliery, T. J., Wilson, C. G. M., Pan, W., Mishler, D., Ghosh, I., Hamilton, A. D., & Regan, L. (2005). Detecting protein-protein interactions with a green fluorescent protein fragment reassembly trap: Scope and mechanism. *Journal of the American Chemical Society*, *127*(1), 146–157. https://doi.org/10.1021/ja046699g

Mahul-Mellier, A.-L., Burtscher, J., Maharjan, N., Weerens, L., Croisier, M., Kuttler, F., … Lashuel, H. A. (2020). The process of Lewy body formation, rather than simply α-synuclein fibrillization, is one of the major drivers of neurodegeneration. *Proceedings of the National Academy of Sciences of the United States of America*, *117*(9). https://doi.org/10.1073/pnas.1913904117

Mbefo, M. K., Fares, M. B., Paleologou, K., Oueslati, A., Yin, G., Tenreiro, S., … Lashuel, H. A. (2015). Parkinson disease mutant E46K enhances α-synuclein phosphorylation in mammalian cell lines, in yeast, and in vivo. *Journal of Biological Chemistry*, *290*(15), 9412–9427. https://doi.org/10.1074/jbc.M114.610774

Mohammadi, S., Nikkhah, M., & Hosseinkhani, S. (2017). Investigation of the effects of carbon-based Nanomaterials on A53T alpha-Synuclein aggregation using a whole-cell recombinant biosensor. *International Journal of Nanomedicine*, *12*, 8831–8840. https://doi.org/10.2147/IJN.S144764

Moussaud, S., Malany, S., Mehta, A., Vasile, S., Smith, L. H., & McLean, P. J. (2015). Targeting α-synuclein oligomers by protein-fragment complementation for drug discovery in synucleinopathies. *Expert Opinion on Therapeutic Targets*, *19*(5), 589–603. https://doi.org/10.1517/14728222.2015.1009448

Outeiro, T. F., Putcha, P., Tetzlaff, J. E., Spoelgen, R., Koker, M., Carvalho, F., … McLean, P. J. (2008). Formation of toxic oligomeric α-synuclein species in living cells. *PLoS ONE*, *3*(4), 1–9. https://doi.org/10.1371/journal.pone.0001867

Paumier, K. L., Sukoff Rizzo, S. J., Berger, Z., Chen, Y., Gonzales, C., Kaftan, E., … Dunlop, J. (2013). Behavioral Characterization of A53T Mice Reveals Early and Late Stage Deficits Related to Parkinson's Disease. *PLoS ONE*, *8*(8). https://doi.org/10.1371/journal.pone.0070274

Prasad, V., Wasser, Y., Hans, F., Goswami, A., Katona, I., Outeiro, T. F., … Voigt, A. (2018). Monitoring α-synuclein multimerization *in vivo*. *The FASEB Journal*, (18), fj.201800148RRR. https://doi.org/10.1096/fj.201800148RRR

Putcha, P., Danzer, K. M., Kranich, L. R., Scott, A., Silinski, M., Mabbett, S., … McLean, P. J. (2010). Brain-Permeable Small-Molecule Inhibitors of Hsp90 Prevent -Synuclein Oligomer Formation and Rescue -Synuclein-Induced Toxicity. *Journal of Pharmacology and Experimental Therapeutics*, *332*(3), 849–857. https://doi.org/10.1124/jpet.109.158436

Reyes, J. F., Rey, N. L., Bousset, L., Melki, R., Brundin, P., & Angot, E. (2014). Alpha-synuclein transfers from neurons to oligodendrocytes. *Glia*, *62*(3), 387–398. https://doi.org/10.1002/glia.22611

Roberts, R. F., Wade-Martins, R., & Alegre-Abarrategui, J. (2015). Direct visualization of alpha-synuclein oligomers reveals previously undetected pathology in Parkinson's disease brain. *Brain*, *138*(6), 1642–1657. https://doi.org/10.1093/brain/awv040

Ruf, V. C., Nübling, G. S., Willikens, S., Shi, S., Schmidt, F., Levin, J., … Giese, A. (2019). Different Effects of α-Synuclein Mutants on Lipid Binding and Aggrefile:///Users/bryanfrey/Downloads/s42003-019-0598-9.pdfgation Detected by Single Molecule Fluorescence Spectroscopy and ThT Fluorescence-Based Measurements. *ACS Chemical Neuroscience*, *10*(3), 1649–1659. https://doi.org/10.1021/acschemneuro.8b00579

Savolainen, M. H., Yan, X., Myöhänen, T. T., & Huttunen, H. J. (2015). Prolyl oligopeptidase enhances α-Synuclein dimerization via direct protein-protein interaction. *Journal of Biological Chemistry*, *290*(8), 5117–5126. https://doi.org/10.1074/jbc.M114.592931

So, P. P. L., Khodr, C. E., Chen, C. Di, & Abraham, C. R. (2013). Comparable dimerization found in wildtype and familial Alzheimer's disease amyloid precursor protein mutants. *American Journal of Neurodegenerative Diseases*, *2*(1), 15–28.

Sulzer, D., & Edwards, R. H. (2019). The physiological role of α-synuclein and its relationship to Parkinson's Disease. *Journal of Neurochemistry*, *150*(5), 475–486. https://doi.org/10.1111/jnc.14810

Tetzlaff, J. E., Putcha, P., Outeiro, T. F., Ivanov, A., Berezovska, O., Hyman, B. T., & McLean, P. J. (2008). CHIP targets toxic α-synuclein oligomers for degradation. *Journal of Biological Chemistry*, *283*(26), 17962–17968. https://doi.org/10.1074/jbc.M802283200

Volpicelli-daley, L. a, Luk, K. C., Patel, T. P., Tanik, S. a, Dawn, M., Stieber, A., … Lee, V. M. (2011). Exogenous α-Synuclein Fibrils Induce Lewy Body Pathology Leading to Synaptic Dysfunction and Neuron Death. *Neuron*, *72*(1), 57–71. https://doi.org/10.1016/j.neuron.2011.08.033.Exogenous

Wang, L., Das, U., Scott, D. A., Tang, Y., McLean, P. J., & Roy, S. (2014). α-Synuclein multimers cluster synaptic vesicles and attenuate recycling. *Current Biology*, *24*(19), 2319–2326. https://doi.org/10.1016/j.cub.2014.08.027

Weinreb, P. H., Zhen, W., Poon, A. W., Conway, K. A., & Lansbury, P. T. (1996). NACP, a protein implicated in Alzheimer's disease and learning, is natively unfolded. *Biochemistry*, *35*(43), 13709–13715. https://doi.org/10.1021/bi961799n

Winner, B., Jappellia, R., Majic, S. K., Desplatsd, P. A., Boyera, L., Aignera, S., … Fred H. Gagea, 4, 5, and Roland Rieka, c, 4, 5. (2011). In vivo demonstration that α-synuclein oligomers are toxic. *PNAS*, *108*(10), 4194–4199. https://doi.org/www.pnas.org/cgi/doi/10.1073/pnas.1100976108

Zheng, Y., Qu, J., Xue, F., Zheng, Y., Yang, B., Chang, Y., … Zhang, J. (2018). Novel DNA Aptamers for Parkinson's Disease Treatment Inhibit α-Synuclein Aggregation and Facilitate its Degradation. *Molecular Therapy - Nucleic Acids*, *11*(June), 228–242. https://doi.org/10.1016/j.omtn.2018.02.011

Zondler, L., Miller-Fleming, L., Repici, M., Gonçalves, S., Tenreiro, S., Rosado-Ramos, R., … Outeiro, T. F. (2014). DJ-1 interactions with a-synuclein attenuate aggregation and cellular toxicity in models of Parkinson's disease. *Cell Death and Disease*, *5*(7), 1–10. https://doi.org/10.1038/cddis.2014.307

Figures

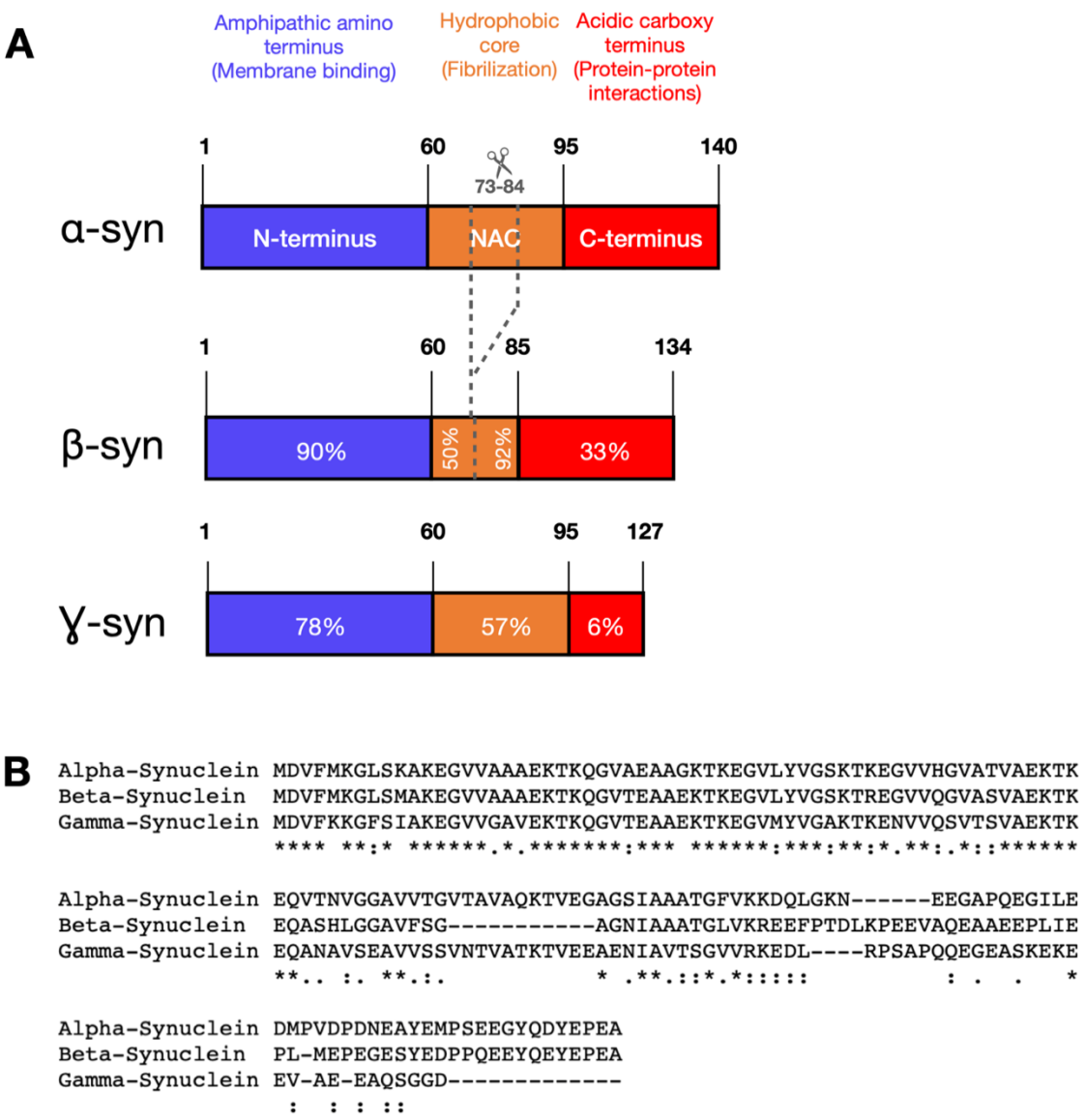

Figure 1: Schematics of α-syn domains and synuclein family members.
A. Schematic of α-syn domains highlighting the similarities in the primary amino acid sequences among the three synuclein family members. **B.** Amino acid sequence alignment of each synuclein family member.

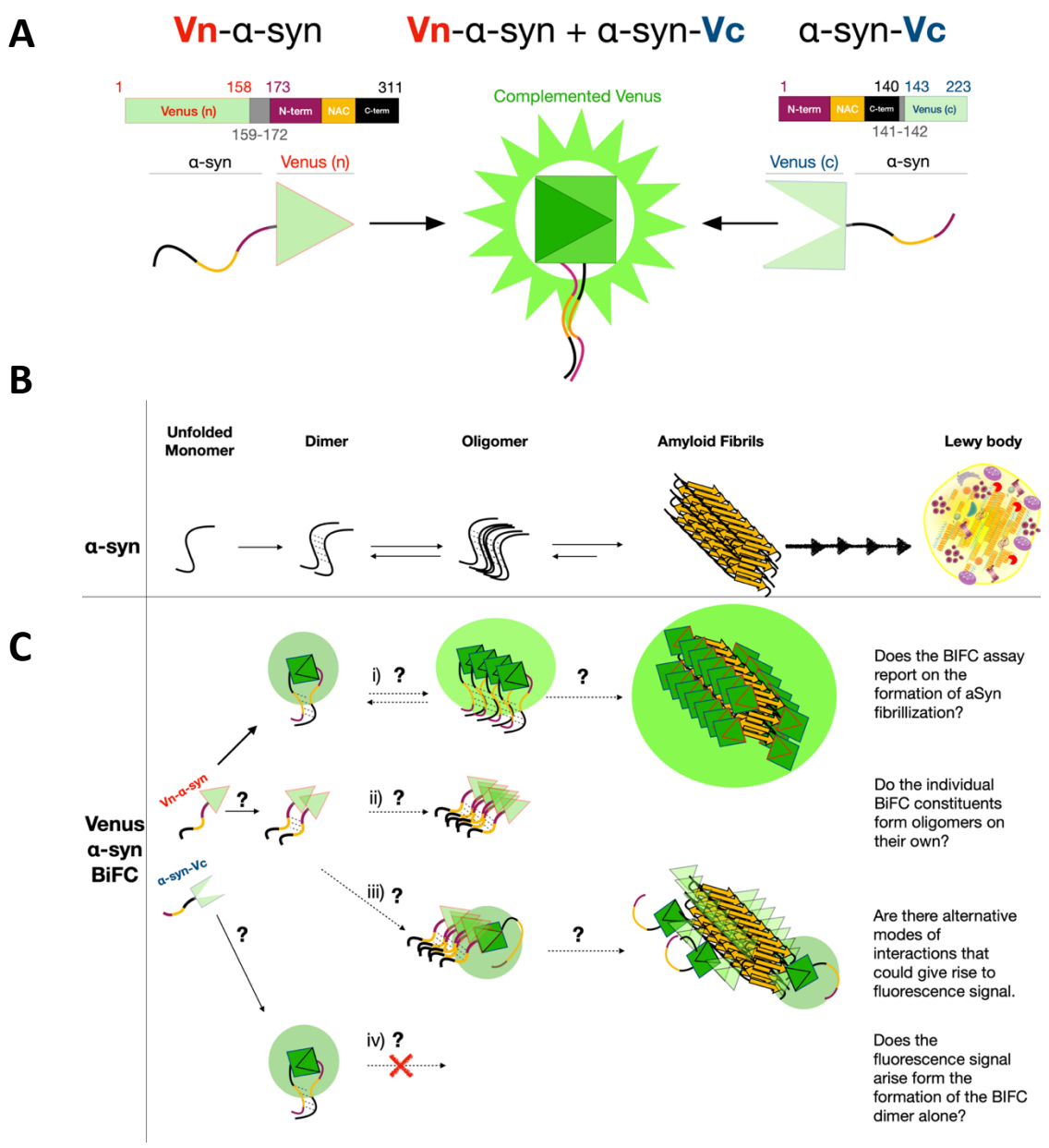

Figure 2: Alpha-synuclein bimolecular fluorescence complementation (BiFC) assays: General principles and outstanding questions. **A.** Schematic depiction of the individual BiFC fragments which emits fluorescence upon α-syn-dimerization/oligomerization mediated reconstitution of the fluorescent protein Venus. **B.** A simplified representation of the mechanism of WT α-syn oligomerization, fibrillization and Lewy body formation **C**. Representation of the various possibilities for homo- and hetero-association between the BiFC fragments and that the scenarios that could lead to the generation of the BiFC fluorescence signal. From top to bottom: i) assumed α-syn BiFC oligomerization model, where the BIFC signal is generated upon α-syn-dimerization/oligomerization mediated reconstitution of the fluorescent protein, Venus. What is not known is whether this dimer is capable of forming higher order oligomers and/or convert to amyloid fibrils similar to α-syn fibrils found in LBs. ii) Possibility that one or both of the two constituents self-oligomerize on their own. iii) illustration of how interactions between one monomeric BiFC constituent with an aggregated/oligomerized species of its counterpart could also give rise to fluorescence signals, which could be wrongly interpreted as being derived from two monomers. iv) Reported drawback of BiFC: the formation of irreversible α-syn dimers with the reconstituted BiFC reporter, which may not exhibit the same biophysical and oligomerization properties of native untagged α-syn. Vn-α-syn: (amino terminal fraction of Venus)-α-syn; α-syn-Vc: α-syn-(carboxy terminal fraction of Venus)

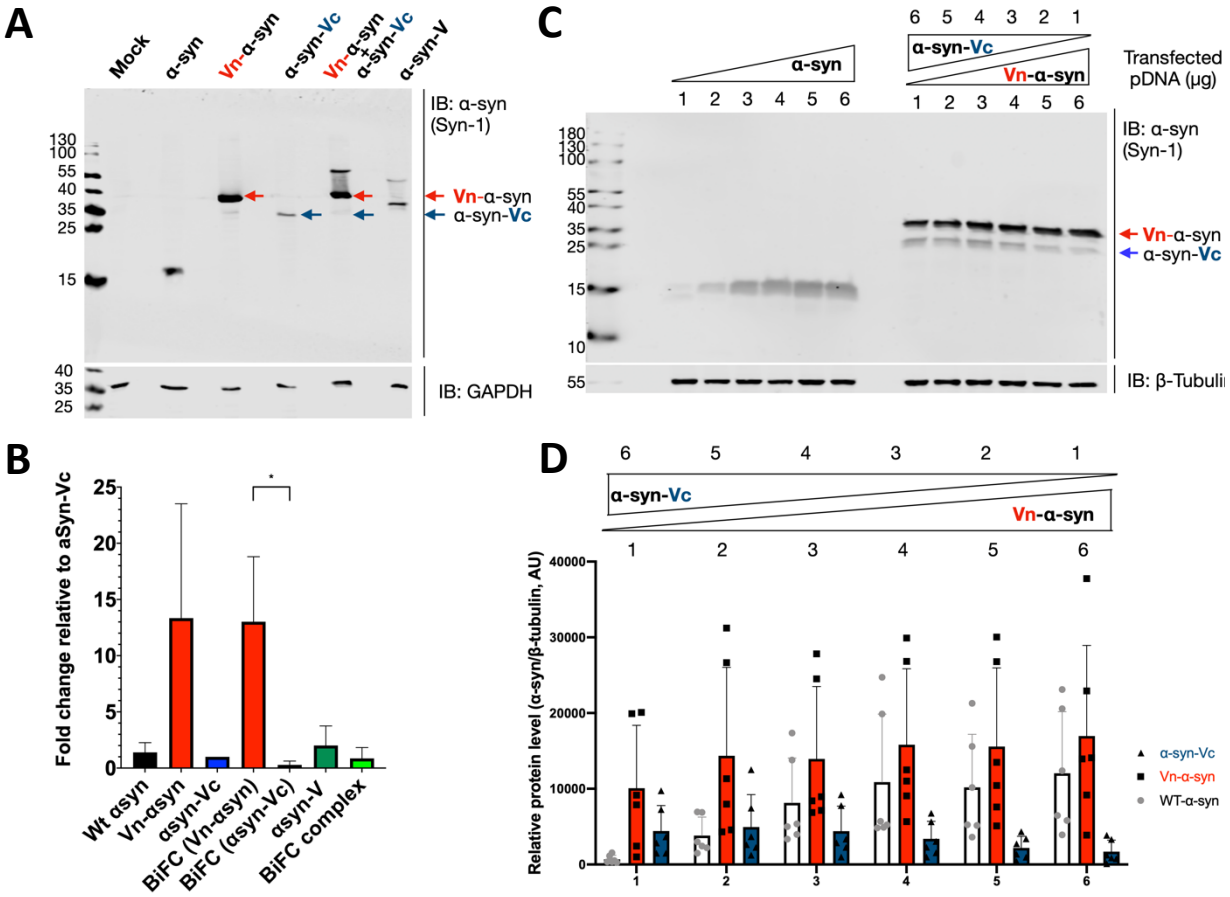

Figure 3: The two BiFC fragment proteins are not expressed at the same level in HEK-293 cells. **A.** HEK-293 cells overexpressing distinct α-syn constructs were lysed 48 h after transfection, and the cell lysates were analyzed by immunoblotting for α-syn (Syn-1), without boiling. GAPDH was used as the loading control. A representative blot of n=3 experiments is shown **B.** Densitometry of data shown in (A.); a significant difference was indicated (p=0.045) by one-way ANOVA followed by a Tukey test for BiFC (Vn-α-syn) vs. BiFC (α-syn-Vc). **C.** WB of lysates from HEK-293 cells transfected with various amounts of vector α-syn DNA (depicted above the blot). α-syn was detected by anti-α-syn (Syn-1). The samples were boiled to disrupt complex formation to allow accurate determination of the levels of the two fragments. **D.** Relative protein levels (α-syn/β-tubulin) of BiFC proteins determined by quantification of the respective bands in (D) using Image Studio Lite. Data are shown as the mean of three independent experiments, each performed as technical duplicates (error bars represent the S.D.). No relevant significant difference was observed between the tested conditions using one-way ANOVA followed by a Tukey test. Vn-α-syn: (amino terminal fraction of Venus)-α-syn; α-syn-Vc: α-syn-(carboxy terminal fraction of Venus); α-syn-V (α-synuclein-Venus full length)

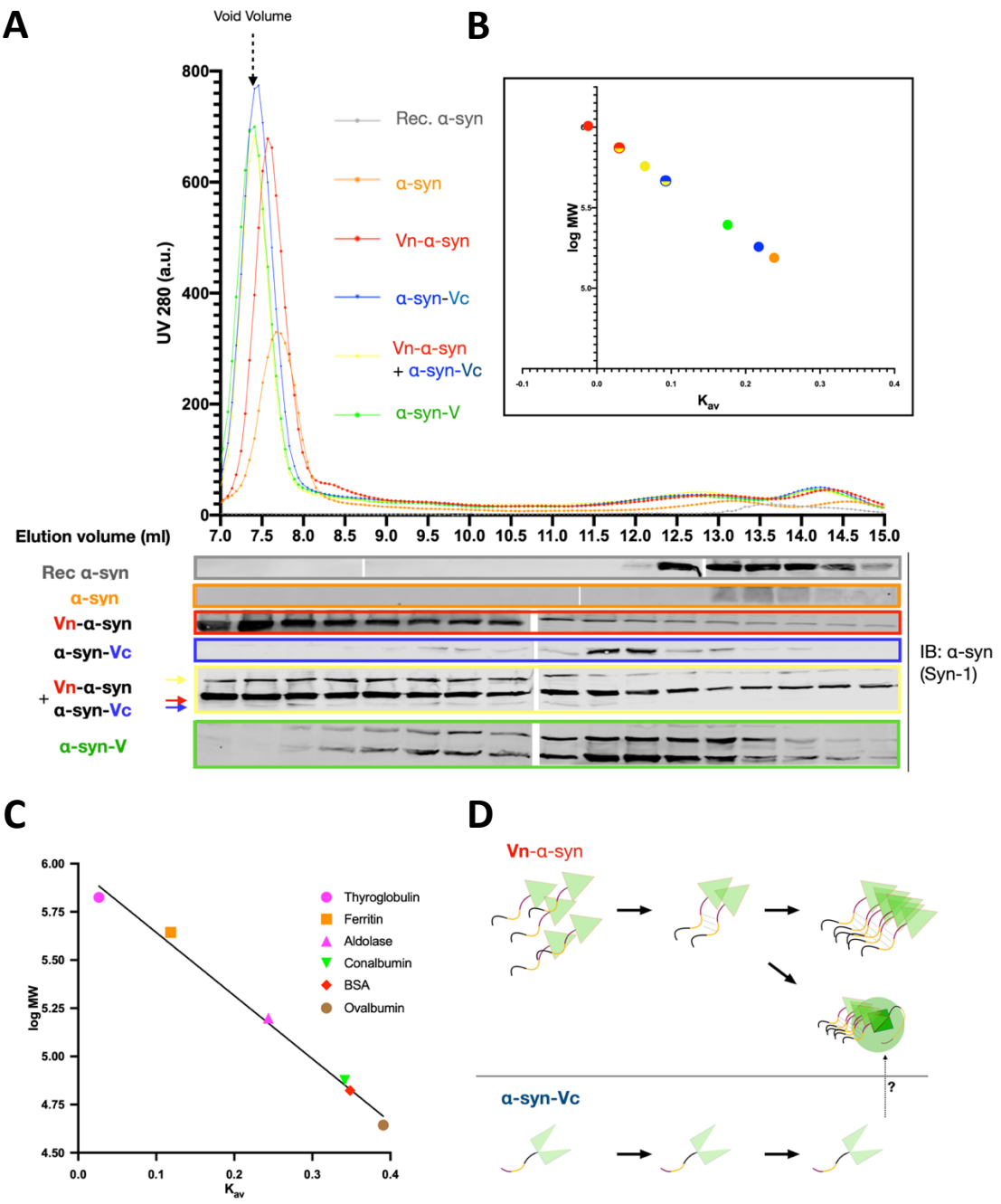

Figure 4: The Vn-α-syn fragment exhibits a high propensity to form soluble oligomers compared to α-syn-Vc and WT α-syn

A. Size exclusion chromatography of a HEK-293 cell lysate 48 h post-transfection with the indicated α-syn constructs. The SEC fractions were analyzed by WB using anti-α-syn (Syn-1) antibodies. **B.** Calculated apparent MW depicted with a log scale plotted against the Kav value of each α-syn construct (large colored dots). **C.** Standard curve generated using the indicated six reference proteins. **D.** Working model suggesting that the high propensity of Vn-α-syn to oligomerize and how such oligomers could interact with or entrap α-syn-Vc. Representative data shown from n=3 experiments. Vo: dead volume; Ve: elution volume; Vn-α-syn: (amino terminal fraction of Venus)-α-syn; α-syn-Vc: α-syn-(carboxy terminal fraction of Venus); α-syn-V (α-synuclein-Venus full length).

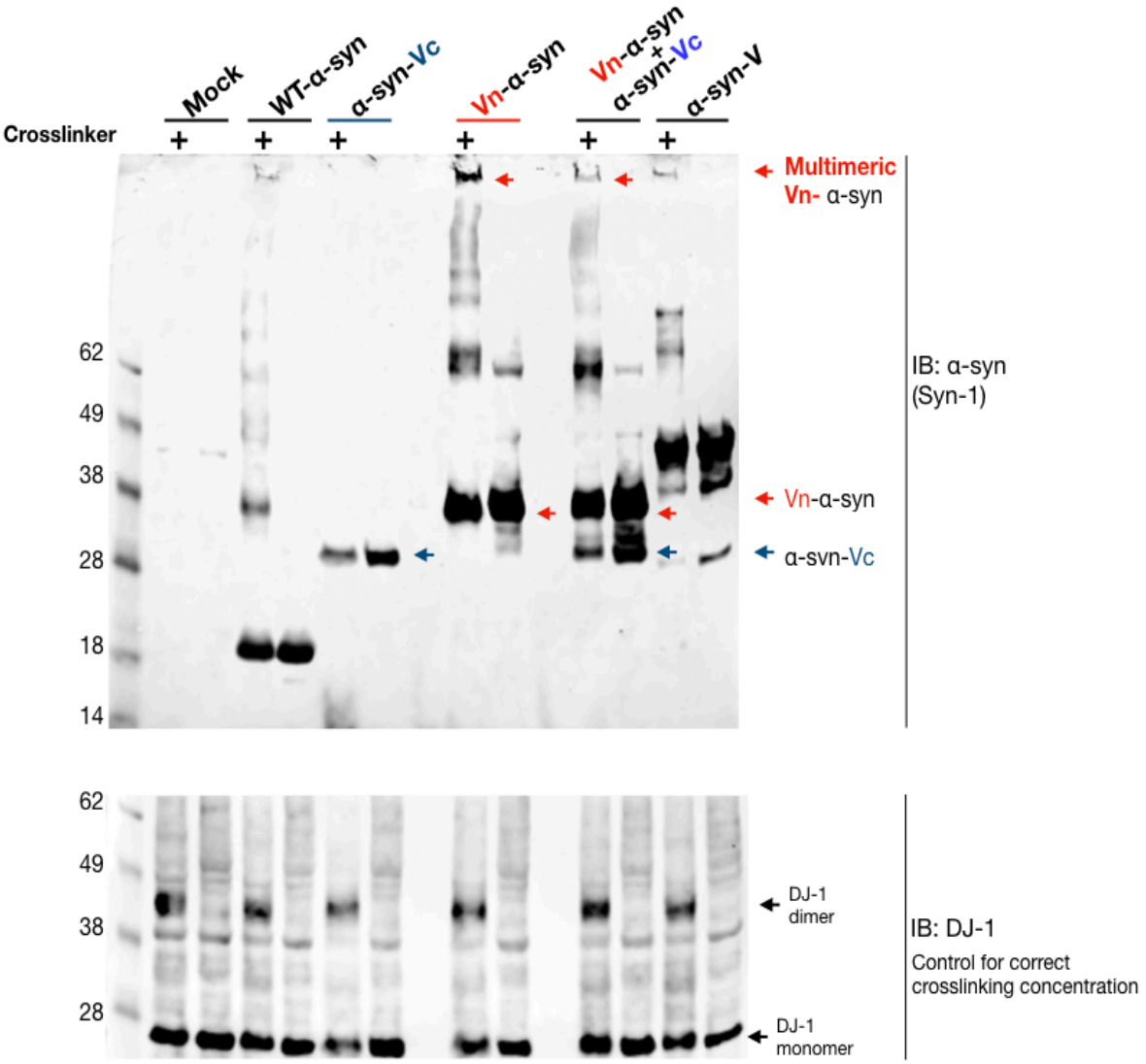

Figure 5: Intact cell crosslinking of α-syn BiFC constructs confirms SEC findings of Vn-α-syn oligomerization

Living HEK-293 cells were crosslinked by the addition of DSG 48 h post transfection with the indicated α-syn constructs, and the resulting cell lysate was analyzed by Western blotting against α-syn using the Syn-1 antibody. The physiological dimer DJ-1 was used as an internal control so that the correct crosslinker concentration was applied. All analyzed α-syn proteins displayed higher MWs upon addition of the DSG crosslinker, except for α-syn-Vc. DJ-1 immunoblotting was used as a control to detect dimers only upon crosslinking. EV: empty vector; Vn-α-syn: (amino terminal fraction of Venus)-α-syn; α-syn-Vc: α-syn-(carboxy terminal fraction of Venus); α-syn-V (α-synuclein-Venus full length). Blots are representative of n=3 experiments.

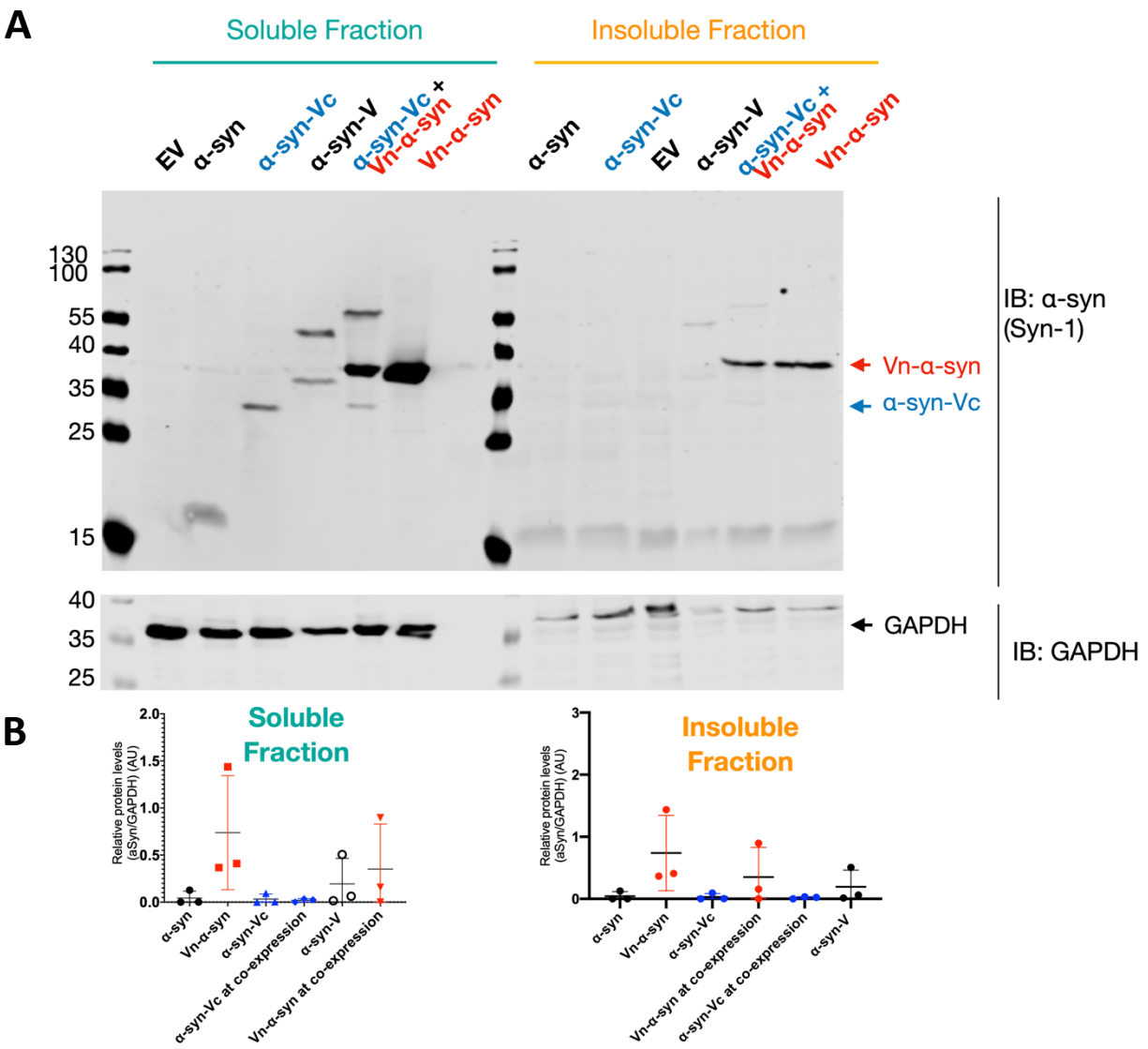

Figure 6: Vn-α-syn, but not α-syn-Vc or WT α-syn, is detected in the insoluble fractions but.
A. HEK-293 cells overexpressing distinct α-syn constructs were lysed 48 h after transfection, and the cell lysates were separated into a soluble and insoluble fraction by centrifugation. The resulting fractions were analyzed by immunoblotting of α-syn (Syn-1). GAPDH was used as the loading control. Shown is a representative blot of n=3 experiments. **B.** Resulting soluble and insoluble band intensities of (A) were quantified and normalized to GAPDH. EV: empty vector; Vn-α-syn: (amino terminal fraction of Venus)-α-syn; α-syn-Vc: α-syn-(carboxy terminal fraction of Venus); α-syn-V (α-synuclein-Venus full length).

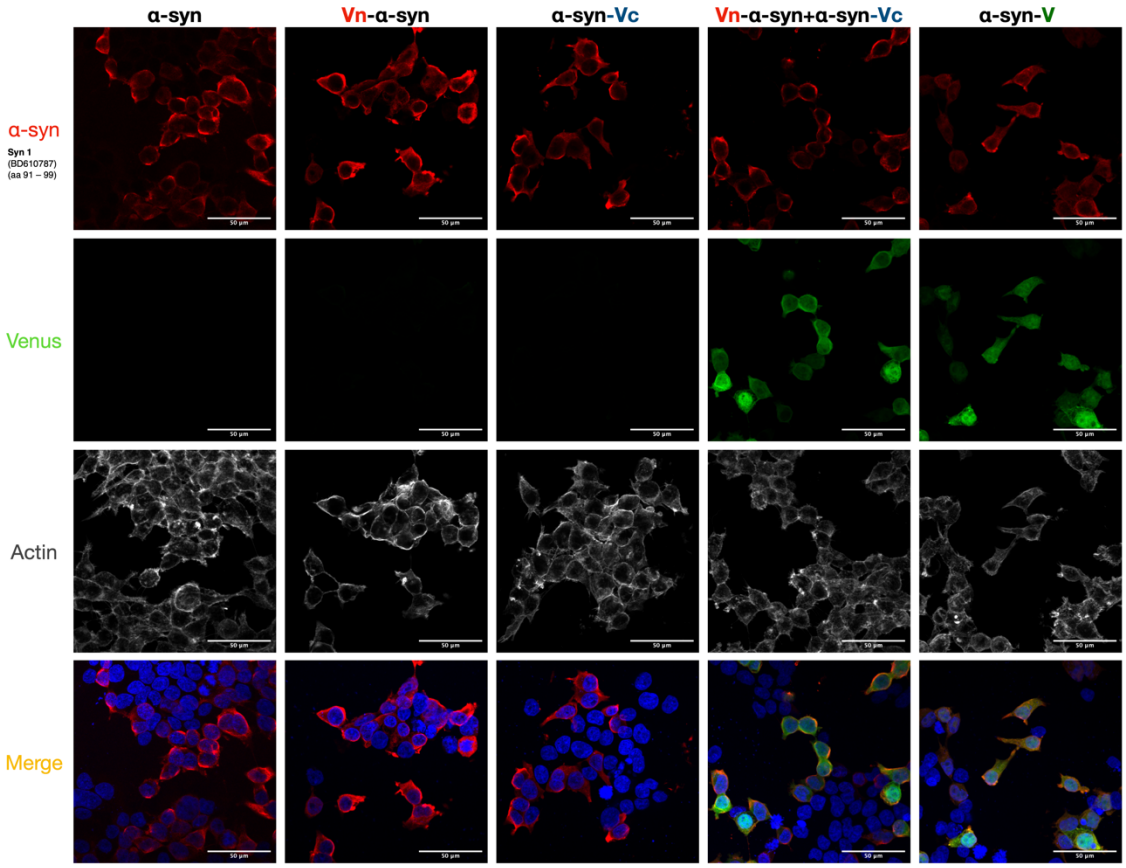

Figure 7: No α-syn inclusion or amyloid-like aggregates were observed in cell lines expressing the BiFC fragments.

HEK-293 cells expressing the indicated α-syn constructs were fixed 48 h post-transfection and stained with the Syn-1 antibody. Upon co-transfection of the Vn-α-syn and α-syn-Vc constructs, Venus was successfully reconstituted and emitted a fluorescent signal that colocalized with the signal for α-syn. To visualize the cells, F-actin was stained with Phalloidin-Atto 565, and the nucleus was counterstained with DAPI. Both α-syn-V and the reconstituted BiFC fragments showed a nuclear localization and signal that did not colocalize with that of α-syn (Syn-1) The scale bar is 50 µm in all images. Shown are representative images from four independent experiments.